Earth Syst. Sci. Data Discuss., https://doi.org/10.5194/essd-2018-29
Manuscript under review for journal Earth Syst. Sci. Data
Discussion started: 19 April 2018

Open Access Earth System Science Data Discussions

Radiocarbon Measurements of Ecosystem Respiration and Soil Pore-Space CO_2 in Utqiaġvik (Barrow), Alaska

Lydia J. S. Vaughn[1,2], Margaret S. Torn[2,3]

[1]Integrative Biology, University of California, Berkeley, Berkeley, CA, 94720, USA
[2]Lawrence Berkeley National Laboratory, Berkeley, CA, 94720, USA
[3]Energy and Resources Group, University of California, Berkeley, Berkeley, CA, 94720, USA

Correspondence to: Lydia J. S. Vaughn (lydiajsvaughn@gmail.com)

Abstract. Radiocarbon measurements of ecosystem respiration and soil pore space CO_2 are useful for determining the sources of ecosystem respiration, identifying environmental controls on soil carbon cycling rates, and parameterizing and evaluating models. We measured flux rates and radiocarbon contents of ecosystem respiration, as well as radiocarbon in soil profile CO_2 in Utqiaġvik (Barrow), Alaska, during the summers of 2012, 2013, and 2014. We found that radiocarbon in ecosystem respiration ranged from +60.5 to -160 ‰ with a median value of +23.3 ‰. Ecosystem respiration became more depleted in radiocarbon from summer to autumn, indicating increased decomposition of old soil organic carbon and/or decreased CO_2 production from fast-cycling carbon pools. Across permafrost features, ecosystem respiration from high-centered polygons was depleted in radiocarbon relative to other polygon types. Radiocarbon content in soil pore-space CO_2 varied between -7.1 and -280 ‰, becoming more negative with depth in individual soil profiles. These pore-space radiocarbon values correspond to CO_2 mean ages of 410 to 3350 years, based on a steady-state, one-pool model. Together, these data indicate that soil respiration is derived primarily from old, slow-cycling carbon pools, but that total CO_2 fluxes depend largely on autotrophic respiration and heterotrophic decomposition of fast-cycling carbon within the shallowest soil layers. The relative contributions of these different CO_2 sources are highly variable across microtopographic features and time in the sampling season. The highly negative $\Delta^{14}C$ values in soil pore-space CO_2 and autumn ecosystem respiration indicate that when it is not frozen, very old soil carbon is vulnerable to decomposition. Radiocarbon data and associated CO_2 flux and temperature data are stored in the data repository of the Next Generation Ecosystem Experiments (NGEE-Arctic) at http://dx.doi.org/10.5440/1364062.

1. Introduction

The flux of CO_2 from ecosystems to the atmosphere is a critical component of the global carbon budget. This flux is highly heterogeneous in space and time, so extensive datasets are needed to evaluate the carbon balance within ecosystems. Many measurements have been made of soil surface CO_2 emissions using soil chambers and eddy covariance towers (e.g., Baldocchi, 2008; Davidson et al., 2002; Norman et al., 1997; Xu and Baldocchi, 2004). Such measurements reveal spatial and temporal patterns in soil and ecosystem respiration that are important for scaling soil carbon emissions across the landscape or identifying drivers of respiration rates (Wainwright et al., 2015). Bulk CO_2 fluxes, however, do not provide information on the cycling rates or relative contributions of different soil carbon pools to total CO_2 emissions. CO_2 emitted from the soil surface includes rapidly cycling carbon in autotrophic respiration as well as heterotrophic decomposition of soil carbon that cycles on broad range of timescales. Shifts in these carbon pool distributions can have large long-term consequences for soil carbon stocks, but may be impossible to detect in bulk CO_2 flux rates (Hopkins et al., 2012; Schuur et al., 2009; Torn et al., 2009; Trumbore, 2000, 2009).

Earth Syst. Sci. Data Discuss., https://doi.org/10.5194/essd-2018-29
Manuscript under review for journal Earth Syst. Sci. Data
Discussion started: 19 April 2018

Linking CO_2 emissions with carbon cycling rates requires a tracer of carbon dynamics that can differentiate between source carbon pools. Natural abundance radiocarbon provides such a tracer, as the radiocarbon content of CO_2 reflects the age (since photosynthesis) and decomposition rates of its component sources (Trumbore, 2000). Accordingly, radiocarbon in surface CO_2 emissions and soil pore gas can be used to quantify carbon cycling rates and assess their variability across space, time, and environmental factors such as thaw depth, soil moisture, temperature, and vegetation (Gaudinski et al., 2000; Trumbore, 2000). Within and across sites, such variations can indicate differences in substrate utilization by microbial decomposers (Borken et al., 2006; Chasar et al., 2000) and shifts between more fast-cycling and slow-cycling substrate pools (Hicks Pries et al., 2013; Hopkins et al., 2012; Schuur et al., 2009). Radiocarbon measurements of soil respiration may be particularly useful for models of the carbon cycle, as a means to determine parameters and evaluate model performance. Similarly, the radiocarbon signature of respiration can be used to constrain the terrestrial signal in top-down carbon cycle analyses (He et al., 2016; Randerson et al., 2002).

In the high latitudes in particular, increased decomposition rates from large, slow-cycling soil carbon pools have the potential to generate an important long-term climate change feedback (Schuur et al., 2015). There, an estimated 1300 Pg of soil carbon has been protected from decomposition by cold temperatures and often frozen or anoxic conditions (Hugelius et al., 2014), factors that are expected to change as climate change warms soils, alters hydrology, and degrades permafrost (ACIA, 2004). In the lower depths of the seasonally thawed active layer, carbon that has historically cycled on millennial timescales may be highly decomposable under aerobic and thawed conditions (Mueller et al., 2015; Strauss et al., 2014; Waldrop et al., 2010). Our current understanding of this old carbon's decomposability, however, is based primarily on CO_2 production rates from laboratory incubations, which may not accurately reflect in situ decomposition dynamics. To quantify in situ decomposition rates, field radiocarbon measurements can be used to differentiate between slow-cycling and fast-cycling carbon. When measured across seasonal and environmental gradients, radiocarbon abundances in soil respiration link these decomposition dynamics to their environmental controls.

In spite of their use in tracing carbon cycle dynamics, only a limited set of radiocarbon data have been published for Arctic ecosystem respiration (e.g., Hardie et al., 2009; Hicks Pries et al., 2013; Lupascu et al., 2014; Phillips et al., 2015) or soil pore-space CO_2 (Czimczik and Welker, 2010; Lupascu et al., 2014a, 2014b), from only a few sites and tundra types. To our knowledge, no data are currently available on radiocarbon in CO_2 from Arctic polygon tundra. Here, we present measurements of radiocarbon in ecosystem respiration and soil pore-space CO_2 from a polygon tundra ecosystem in Utqiaġvik, Alaska. We measured rates and radiocarbon contents of soil surface CO_2 emissions across three summer seasons, from a range of ice wedge polygon features. Using soil pore-space $^{14}CO_2$ profiles, we quantified vertical distributions of carbon cycling rates within the soil profile. Together, these measurements reveal temporal patterns and spatial relationships in ecosystem respiration and its source carbon pools.

2. Study Site

Field sampling was conducted at the Barrow Environmental Observatory (BEO), ~6 km east of Utqiaġvik (formerly Barrow), Alaska (71.3 °N, 156.5 °W), at the northern end of the Alaskan Arctic coastal plain. Utqiaġvik has a mean annual temperature of -12 °C and mean annual precipitation of 106 mm, with long, dry winters and short, moist, cool summers. The land surface has low topographic relief reaching a maximum elevation of 5 m (Brown et al., 1980; Hubbard et al., 2013). The seasonally-thawed active layer ranges from 20 to 60 cm, underlain by continuous ice-rich permafrost to depths greater than 400 m (Hinkel and

Nelson, 2003). Formed from the late Pleistocene Gubic formation (Black, 1964), soils in the region are dominated by Typic Aquiturbels (53 %), Typic Histoturbels (22 %), and Typic Aquorthels (8.6 %) (Bockheim et al., 1999).

Within the BEO, ~65 % of the ground surface is covered by ice wedge polygons (Lara et al., 2014), discrete landscape units formed by the growth and degradation of subsurface ice wedges (Billings and Peterson, 1980; Brown et al., 1980). Individual polygons are 10-20 m in diameter with raised, relatively dry rims at their perimeter and are separated by low-lying, saturated troughs. Polygons can be classified according to the elevation of their centers; low-centered polygons (LC) have standing water and primarily graminoid vegetation while high-centered polygons (HC) have dry surface soils and a greater abundance of mosses and lichens. Between HC and LC polygons, flat-centered polygons (FC) have intermediate morphology and subsurface properties. Among LC, FC, and HC polygons, differences in active layer depth, oxygen availability, soil carbon distribution, and thermal conductivity (Liljedahl et al., 2016; Lipson et al., 2012; Ping et al., 1998) create strong differences in surface carbon fluxes (Vaughn et al., 2016; Wainwright et al., 2015). To capture this range of microtopography and associated carbon cycle controls, we collected CO_2 samples from centers, rims, and troughs of the three polygon types.

3. Field Measurements and Sample Collection

3.1 Surface CO_2 Emissions

In August and October 2012, July and September 2013, and September 2014, we collected soil surface CO_2 emissions for radiocarbon analysis using a static chamber method modified from Hahn et al. (2006). Samples were collected from a total of 19 locations within 11 polygons (4 LC, 4 FC, 3 HC). Opaque chambers (25 cm diameter) were seated on circular PVC chamber bases extending to depths of ~10 cm below the soil surface. We installed all bases at least two days prior to sampling to limit the influence of disturbance on gas flux rates and radiocarbon values. Based on variations in the surface and depths of bases, aboveground chamber height varied between ~15 and 20 cm. Chambers blocked light transmission and were tall enough to enclose surface vegetation, so CO_2 emissions were equivalent to ecosystem respiration. For sample collection, the chamber was placed in a 3 cm-deep channel on the top rim of each base, which was filled with water to create an airtight seal. We then circulated chamber gas through soda lime for 20 minutes at a flow rate of 1 L min^{-1} to remove ambient CO_2. CO_2 was allowed to accumulate in the chamber over 2 to 48 hours, depending on the rate of CO_2 accumulation, which we monitored periodically by passing a 30 mL sample of chamber gas through a LI-820 CO_2 gas analyzer (LI-COR) at a flow rate of ~1 L min^{-1}. For all samples, the final chamber CO_2 concentration was more than twice its initial concentration, important for accuracy in chamber radiocarbon measurements (Egan et al., 2014). Based on this concentration measurement, a volume of chamber gas sufficient for radiocarbon analysis was collected in one or more 500-1000 mL evacuated stainless steel canisters connected by capillary tubing to a chamber sampling port. High-concentration samples were collected with a syringe and needle through a septum in the sampling port and immediately injected into evacuated glass vials sealed with 14 mm-thick chlorobutyl septa (Bellco Glass, Inc.). To correct chamber gas samples for atmospheric contamination, we collected local air samples in 3000 mL stainless steel canisters on August 12, 2012, July 13, 2013, and September 2 and 7, 2014.

In July and September 2013 and September 2014, we measured rates of ecosystem respiration from radiocarbon sampling locations. CO_2 fluxes were measured within 2 days of radiocarbon sample collection, using opaque static chambers seated on bases described above and vented according to Xu et al. (2006) to minimize pressure changes due to the Venturi effect. For each measurement, we measured CO_2 concentrations within the chamber over a period of 4-8 minutes using a Los Gatos Research, Inc. Portable Greenhouse Gas Analyzer. We calculated the CO_2 flux rate (equivalent to ecosystem respiration) as the slope of

the linear portion of its concentration vs. time curve, converted to units of μmol m^{-2} s^{-2} according to chamber volume and temperature. Endpoints of this linear region were determined manually for each curve, and measurements lacking a clear linear range were not included in the dataset. Corresponding with each CO_2 flux measurement, we measured thaw depth with a tile probe.

3.2. Soil Pore-Space CO_2

In August 2012 and July 2013, we collected soil pore gas from a total of 6 soil profiles within 5 polygons (1 LC, 2 FC, 2 HC). Samples were collected with a method similar to Czimczik and Welker (2010). Briefly, 1/4" diameter stainless steel probes were inserted into the soil at 45 ° angles to vertical depths of 10, 20, and 30 cm, or to 2 cm above the frost table if thaw depth was less than 30 cm. Probes were capped with gastight septa and allowed to remain in place throughout the sampling season. Before collecting each sample, we purged 10 mL of gas from the probe and measured the CO_2 concentration with a LI-820 CO_2 gas analyzer as described above. Radiocarbon samples were collected by connecting evacuated 500-1000 mL stainless steel canisters to probes via flow-restricting tubing (Upchurch scientific, 0.01" ID × 10 cm length), which allowed canisters to fill slowly over 4 hours with minimal disturbance to the soil CO_2 concentration gradient (Gaudinski et al., 2000). In-line Drierite water traps were used during sample collection to prevent moisture accumulation in canisters. As with surface respiration samples, high-concentration samples were collected from probes with a syringe and needle and immediately injected into evacuated glass vials. Due to water-saturated soils or clogged soil probes, we were unable to obtain samples from all profiles and depths. For this reason, the final sample set represents only a subset of depths and sampling locations.

3.4. Sample Purification and Radiocarbon Analysis

CO_2 from gas samples was cryogenically purified under vacuum, divided for ^{14}C and ^{13}C analysis, and sealed in 9 mm quartz tubes. For radiocarbon analysis, we sent samples to Lawrence Livermore National Laboratory's Center for Accelerator Mass Spectrometry (CAMS) or the Carbon, Water, and Soils Research Lab at the USDA-FS Northern Research Station, where CO_2 was reduced to graphite on iron powder under H_2. ^{14}C abundance was then measured at CAMS using an HVEC FN Tandem Van de Graaff accelerator mass spectrometer or at UC Irvine's Keck Carbon Cycle AMS facility. $^{13}C/^{12}C$ in CO_2 splits was analyzed on the UC Davis Stable Isotope Laboratory GVI Optima Stable Isotope Ratio Mass Spectrometer.

Following the conventions of Stuiver and Polach (1977), radiocarbon results are presented as fraction modern relative to the NBS Oxalic Acid I (OX1) standard ($F^{14}C$), and deviations in parts per thousand (‰) from the absolute (decay-corrected) OX1 standard ($\Delta^{14}C$). All results have been corrected for mass-dependent isotopic fractionation using ^{13}C measurements.

4. Calculations and Data Quality Control

We corrected surface-chamber radiocarbon measurements for atmospheric contamination using the method described in Schuur and Trumbore (2006). Briefly, we determined fractional contributions of background atmosphere and ecosystem respiration to total chamber gas using ^{13}C values in a two-pool mixing model:

$$^{13}C_S = f_{Reco} \times {}^{13}C_{Reco} + f_{atm} \times {}^{13}C_{atm}\,, \quad (1)$$

$$f_{Reco} + f_{atm} = 1\,, \quad (2)$$

where, f_{Reco} and f_{atm} are the fractional contributions of ecosystem respiration and background atmosphere, $^{13}C_S$ and $^{13}C_{atm}$ are the measured ^{13}C abundances in the sample and background atmosphere in units of atom %, and $^{13}C_{Reco}$ is the ^{13}C abundance in ecosystem respiration, approximated separately for each polygon type as the mean ^{13}C of chamber CO_2 samples with $[CO_2]$ > 4000 ppm. To minimize error due to large proportions of atmospheric CO_2, we omitted samples with f_{Reco} < 0.5. For each sample, we calculated $\Delta^{14}C$ of ecosystem respiration ($\Delta^{14}C_{Reco}$) according to Eq. (3):

$$\Delta^{14}C_S = f_{Reco} \times \Delta^{14}C_{Reco} + f_{atm} \times \Delta^{14}C_{atm}\,, \quad (3)$$

where $\Delta^{14}C_S$ and $\Delta^{14}C_{atm}$ are the measured $\Delta^{14}C$ values of the sample and background atmosphere, and f_{Reco} and f_{atm} were calculated from Eq. (1) and Eq. (2). Errors due to analytical precision and variations in source isotopic signatures were propagated through this correction according to the formulation in Phillips and Gregg (2001).

Soil surface CO_2 flux measurements were assessed for quality using two criteria, the standard error of the slope (SE) and the per cent relative standard error (PRSE), defined as $100 \times SE_{slope}/Estimate_{slope}$. Flux measurements with SE > 0.05 and PRSE > 5 were omitted from the dataset. This set of dual criteria avoided biasing the dataset toward low fluxes (if SE alone were used) or high fluxes (if PRSE alone or R^2 were used).

With soil pore-space radiocarbon data, we omitted measurements with CO_2 concentrations less than 400 ppm due to possible leakage and atmospheric contamination during sampling, with the exception of one sample from 31 cm depth with highly negative $\Delta^{14}C$, indicating a low proportion of atmospheric CO_2. At this field site, ^{13}C abundances in pore-space CO_2 vary greatly due to isotopic fractionation from methane production and consumption (Vaughn et al., 2016). For this reason, we could not correct subsurface samples for atmospheric CO_2. Reported radiocarbon values thus represent the total CO_2 present in the soil pore-space, sourced from heterotrophic respiration, root respiration, and downward atmospheric diffusion.

With soil-profile CO_2 samples, we used radiocarbon measurements to model the mean age of carbon in respired CO_2 using the time-dependent steady state turnover time model described in Torn et al. (2009), modified to account for carbon residence time in plant tissues:

$$F'_{C,t}C_t = IF'_{atm,t-T_R} + C_{t-1}F'_{C,t-1}\left(1 - \frac{1}{\tau} - \lambda\right), \quad (4)$$

where:

$F' = \frac{\Delta^{14}C}{1000} - 1$

$F'_C = F'$ of the given carbon pool, equal to F' of the CO_2 sample

$F'_{atm} = F'$ of CO_2 in the local atmosphere

I = input rate of carbon from the atmosphere to the given carbon pool (g C y^{-1})

C = stock of carbon in the given carbon pool (g)

τ = turnover time of the given carbon pool, equivalent to the mean age of carbon in its decomposition flux (y)

λ = radioactive decay rate of ^{14}C (1/8267 y)

T_R = mean residence time of carbon in plants before entering soil organic matter (y).

Earth Syst. Sci. Data Discuss., https://doi.org/10.5194/essd-2018-29
Manuscript under review for journal Earth Syst. Sci. Data
Discussion started: 19 April 2018

At steady state, $C_t = C_{t-1} = I \times \tau$, so Eq. (4) reduces to:

$$F'_{C,t} = \frac{1}{\tau} F'_{\mathrm{atm},t-T_R} + F'_{C,t-1}(1 - \frac{1}{\tau} - \lambda)\,. \quad (5)$$

Following Eq. (5), the $\Delta^{14}C$ value of CO_2 at time *t* thus depends on the turnover time of carbon in the decomposing carbon pool, the mean residence time of carbon in plant material, and the $\Delta^{14}C$ of atmospheric CO_2 in the current and previous year, which has changed continuously since the release of radiocarbon into the atmosphere from nuclear weapons testing between 1950 and the mid 1960s (Trumbore, 2000). This model assumes that CO_2 is derived from a homogeneous pool of decomposing carbon, such that the turnover time of this pool is equal to the mean age of its decomposition flux (Sierra et al., 2017).

The mean residence time of carbon in plants reflects a mixture of materials with varying transfer rates. Some photosynthates enter the soil within 1 day of fixation (Loya et al., 2002), whereas carbon resides in longer-lived plant organs from ~2 to as long as 15 years before entering the soil organic matter pool (Billings et al., 1978; Dennis, 1977). We assumed that across plant organs, plant species, and seasons, the mean value of T_R lies between 0 and 5 years.

Annual atmospheric $\Delta^{14}C$ values were compiled from our data and three other sources: the IntCal13 dataset (Reimer et al., 2013), measurements from Fruholmen, Norway between 1962-1991 (Nydal and Lövseth, 1996), measurements from Utqiaġvik between 1999-2007 (Graven et al., 2012), and our measurements from the BEO in 2012, 2013, and 2014 (Table S1, Fig. S1). From roughly the same latitude as Utqiaġvik, Fruholmen $\Delta^{14}C$ measurements provide a close approximation for missing Utqiaġvik data (Meijer et al., 2008). Because ecosystem CO_2 uptake occurs primarily during the growing season, we averaged June-August $\Delta^{14}C$ values to produce an annualized summer dataset. Data gaps from 1992-1998 and 2008-2011 were filled using an exponential interpolation constrained by the available data from the 10 years surrounding each gap.

Using our measured $\Delta^{14}C$ values and annually resolved atmospheric $\Delta^{14}C$ data, we iteratively solved for the mean age of each CO_2 sample. We performed this calculation twice, using T_R values of 0 and 5 to bracket the likely T_R range. Samples containing a large percentage of recently fixed carbon yielded two possible solutions for each T_R value (Trumbore, 2000). In such cases, we chose the appropriate solution either by comparing the two values to other (unique) mean age values within the same profile, or by comparing the measured carbon stock with the carbon stocks calculated from the CO_2 production rate and the candidate solutions (Torn et al., 2009).

3. Results and Discussion

3.1 Radiocarbon in Ecosystem Respiration

Radiocarbon contents of soil surface CO_2 emissions, equivalent to ecosystem respiration ($\Delta^{14}C_{Reco}$), ranged from +60.5 to -160 ‰, with a median value of +23.3 ‰ (Table 1). The positive $\Delta^{14}C_{Reco}$ values measured in 28 of the 37 samples indicate high proportions of carbon fixed since 1950, likely sourced from both autotrophic respiration and decomposition of rapidly cycling soil carbon in shallow soil layers. In contrast, the negative values measured in the other 9 samples show that the sources of CO_2 were dominated by carbon that cycles on centennial to millennial timescales. $\Delta^{14}C_{Reco}$ followed a left-skewed distribution, with notably negative $\Delta^{14}C_{Reco}$ values measured from LC1-center in October 2012 (-159.5 ‰) and HC1-center in September 2013 (-115.5 ‰). The variations in these $\Delta^{14}C_{Reco}$ values reflect differences in the relative CO_2 production and transport rates from both autotrophic and heterotrophic source pools, whose decomposition rates and radiocarbon contents vary spatially and temporally

(Nowinski et al., 2010). Together, seasonal variations in soil thaw depths and spatial variations in soil organic carbon ^{14}C depth profiles affect the radiocarbon signature of surface CO_2 emissions.

We observed a general decrease in $\Delta^{14}C_{Reco}$ as the sampling season progressed (Fig. 1). This seasonal decline in $\Delta^{14}C_{Reco}$ is consistent with other data from high latitude sites (Hicks Pries et al., 2013; Trumbore, 2000) and reflects seasonal changes in thaw depth, soil temperature, and vegetation activity. Surface soils at this site begin to thaw in June, typically reaching their maximum temperatures in July (Hinkel et al., 2001; Torn, 2015). As shallow soils warm and plant activity increases in this early summer period, ecosystem respiration includes high proportions of ^{14}C-enriched CO_2 from autotrophic respiration and heterotrophic decomposition of shallow, rapid-cycling soil carbon. Later in summer and into the autumn, the balance of respiration shifts toward increased importance of deeper soil decomposition. Autotrophic respiration peaks in July or August, and decreases substantially into the fall after plants senesce (Hicks Pries et al., 2013). During the autumn season, surface soils refreeze while deep soils continue to warm (Table 1) (Zona et al., 2016), limiting heterotrophic respiration from shallow soils while enhancing decomposition from deeper, more ^{14}C-depleted soil carbon pools. The effect of these changes is a seasonal shift in respiration from primarily shallow, fast-cycling source carbon pools to more deep, ^{14}C-depleted soil organic matter.

Across time-series measurements from individual profiles or polygon types, $\Delta^{14}C_{Reco}$ varied not only with time in the sampling season but also with polygon type (Table 1, Fig. 1). HC polygons displayed particularly strong seasonal trends in $\Delta^{14}C_{Reco}$; in each HC polygon from which multiple measurements were made, $\Delta^{14}C_{Reco}$ decreased throughout the summer months to a minimum value in September or October. The magnitude of this seasonal decrease varied greatly among individual HC polygons and microtopographic positions within the polygons, reaching a minimum $\Delta^{14}C_{Reco}$ value of -115 ‰ from the center of polygon HC1 but only +13 ‰ from the trough of HC3 (Table 1). In contrast with HC polygons, $\Delta^{14}C_{Reco}$ from FC and LC polygons remained closer to atmospheric values throughout the sampling season (Fig. 1). One exception was one highly negative $\Delta^{14}C_{Reco}$ value measured in October from the center of polygon LC1. In this instance, with October thaw depths close to their annual maximum, thaw may have penetrated into the transition layer at the top of the permafrost, exposing old, previously frozen carbon to decomposition. Alternatively, this isolated measurement of ^{14}C-depleted CO_2 may reflect heterogeneity within the active layer due to cryoturbation (Kaiser et al., 2007; Ping et al., 1998).

The influence of microtopography on old carbon emissions was particularly apparent in September 2014 (Fig. 2). At this time, decomposition of old carbon consistently dominated the respiration flux from HC polygon centers ($\Delta^{14}C_{Reco}$ = -51.6 ± 32.4 ‰), whereas fast-cycling pools dominated respiration from FC and LC polygon centers (13.0 ± 10.9 ‰ and 5.9 ± 5.6 ‰ respectively). Unlike $\Delta^{14}C_{Reco}$, concurrent ecosystem respiration rates were comparable across the three polygon types (Fig. 2b), which indicates that absolute rates of old carbon decomposition were greater from HC polygons than from LC or FC polygons. Interestingly, soil thaw at this time was deepest in FC polygons (Table 1); across profiles at the site scale, we saw no correlation between thaw depth and $\Delta^{14}C_{Reco}$. This finding suggests that the relationship between the depth of thaw and old carbon mineralization depends on the scale of observation. At the scale of an individual profile, seasonal variations in $\Delta^{14}C_{Reco}$ correspond with changes in thaw depth. At the site scale, however, thaw depth may not be a useful predictor of spatial variations in $\Delta^{14}C_{Reco}$.

In July and September 2013 and September 2014, ecosystem respiration ranged between 0.32 and 2.5 μmol CO_2 m^{-2} s^{-1} (Table 1). The relationship between the rate and radiocarbon content of ecosystem respiration was highly variable (Fig. 3), but with two notable patterns across all data. As ecosystem respiration increased, the variance of $\Delta^{14}C_{Reco}$ tended to decrease, and there were

Earth Syst. Sci. Data Discuss., https://doi.org/10.5194/essd-2018-29
Manuscript under review for journal Earth Syst. Sci. Data
Discussion started: 19 April 2018

no negative $\Delta^{14}C_{Reco}$ measurements associated with fluxes above 1 µmol CO_2 m^{-2} d^{-1} (Fig. 3). These patterns reflect the sensitivity of ecosystem respiration to the most dynamic carbon sources, autotrophic respiration and shallow soil carbon mineralization. Autotrophic respiration can contribute as much as 70 % of ecosystem respiration at the peak of the growing season (Hicks Pries et al., 2013), declining markedly as plants senesce. Similarly, heterotrophic decomposition rates are both highest and most temporally variable in shallow soil layers (Hicks Pries et al., 2013), where soil temperatures exhibit a large seasonal range. As a result, old, slow-cycling carbon from deep soil respiration comprises a large percentage of the total carbon flux only when ecosystem respiration rates are low.

3.2 Radiocarbon in Soil Pore-Space CO_2

At a subset of locations and sampling dates, we measured the radiocarbon content of CO_2 in soil pore gas ($\Delta^{14}C_{CO2p}$). $\Delta^{14}C_{CO2p}$ became increasingly negative with depth in the soil, but varied widely among profiles and sampling dates from -7.1 to -280 ‰ (Table 2, Fig. 4). These negative values indicate that pore-space CO_2 was derived primarily from older soil organic matter, with minimal contributions from plant-respired carbon or fast-cycling soil organic carbon. In general, ecosystem respiration was enriched in radiocarbon relative to soil pore-space CO_2, even at only 10 cm depth (Table 1, Table 2). This observation suggests that the shallowest CO_2 sources—autotrophic respiration and/or heterotrophic decomposition of fast-cycling (annual-decadal) organic carbon—contribute large proportions of the total respiration flux, even late in the season when plants have largely senesced. Detecting and characterizing the decomposition of older, deeper soil organic carbon requires direct measurements of soil pore-space CO_2.

In three soil profiles (HC3-trough, HC3-center, and FC2-center), respired CO_2 became enriched in radiocarbon near the permafrost table (Fig. 2), a pattern that has been previously observed in the Arctic (Lupascu et al., 2014a). In these three profiles, concentrations of CO_2 in deep pore-space samples were 6 to 25 times higher than background atmosphere, so we infer that the higher $\Delta^{14}C_{CO2p}$ values at depth were not caused by downward transport of atmospheric CO_2. Instead, this pattern indicates significant CO_2 production from fast-cycling carbon near the permafrost table. As in other Arctic sites, this depth trend is likely due either to cryoturbation (Bockheim and Tarnocai, 1998) or DOC leaching (Lupascu et al., 2014a), both of which can transport recently fixed, relatively decomposable carbon to the deep section of the active layer.

With $\Delta^{14}C_{CO2p}$ values, we used a single pool turnover time model to calculate the mean age of pore-space CO_2 (Table 2). This model assumes that CO_2 is respired from a homogeneous pool of decomposing carbon (Trumbore, 2000) such that the turnover time equals the mean age of the respired carbon (Sierra et al., 2017). Across all measurement dates and depths, we found the mean age of respired CO_2 ranged from 410 y in one 10 cm sample to 3350 y at only 20 cm depth, indicating decomposition of old and/or slow-cycling carbon, even in relatively shallow soils. HC polygon centers produced particularly old CO_2, with ages greater than 3000 y from HC3-center in July 2013 and HC1-center in August 2012 and September 2013. This observation aligns with the spatial patterns we observed in surface CO_2 emissions, which were particularly ^{14}C-depleted in HC polygons (Table 1, Fig. 1). Together, these findings suggest that low $\Delta^{14}C_{Reco}$ from HC polygon centers was due to mineralization of very old carbon at depth.

Our findings of consistently negative $\Delta^{14}C$ values from soil pore-space CO_2 are similar to those from the other Arctic sites where it has been measured (Czimczik and Welker, 2010; Lupascu et al., 2014b, 2014a). In contrast, studies in temperate or tropical sites find $\Delta^{14}C_{CO2p}$ values that are more similar to atmospheric values (Borken et al., 2006; Gaudinski et al., 2000; Trumbore, 2000), where soil respiration is dominated by root respiration and decomposition of rapidly cycling soil organic matter. This

difference may be due in part to differences among biomes in rooting distributions. Because of strong vertical gradients in soil temperature and nutrient and water availability, rooting distributions in Arctic tundra are extremely shallow (Iversen et al., 2015), limiting most root respiration to the shallow organic layer. Additionally, such negative $\Delta^{14}C_{CO2p}$ values suggest that old, slow-cycling organic matter in Arctic soils is readily decomposable under thawed conditions. Cold soil temperatures and frozen conditions limit microbial activity throughout much of the year, allowing otherwise-decomposable soil organic matter to accumulate. During the short season in which Arctic soils are thawed, these large pools of ^{14}C-depleted soil carbon may be largely unprotected against microbial mineralization. Compared with tropical or temperate soils, existing Arctic soil carbon stores may thus be particularly vulnerable to soil thaw and active layer deepening due to climate change.

Due to sampling limitations, soil profile ^{14}C data are available from only a subset of polygon types and positions. No samples were collected from polygon rims, and only few samples were obtained where soils were saturated (Table 2). For this reason, our dataset does not capture microtopographic variations in deep soil decomposition rates and controls. Soil temperature profiles, vegetation, and soil pore-space oxygen availability influence microbial activity and vary among profiles and with time in the thawed season (Lipson et al., 2012; Olivas et al., 2011). To characterize the relationships between these variables and soil carbon decomposition rates, further measurements are needed of ^{14}C in soil pore-space DIC and CO_2, across spatial, seasonal, and hydrological gradients.

Data Availability

Data are stored in the Next-Generation Ecosystem Experiments (NGEE-Arctic) data repository (Vaughn et al., 2018) and may be accessed at http://dx.doi.org/10.5440/1364062. The code used to generate plots and correct chamber samples for atmospheric contamination can be found at https://github.com/lydiajsvaughn/Radiocarbon_field_Barrow. The code used for turnover time modeling can be found at https://github.com/lydiajsvaughn/Radiocarbon_inc_2012.

Conclusions

We measured the radiocarbon contents of ecosystem respiration and soil pore-space CO_2 between 2012 and 2014 in Utqiaġvik, Alaska. As a naturally occurring tracer of soil carbon dynamics, radiocarbon in CO_2 and soil carbon reflects the rates at which carbon cycles through plant and soil pools (Trumbore, 2000). Radiocarbon provides a powerful tool to test and parameterize models (He et al., 2016) and evaluate how environmental variables, seasonal changes, and disturbance influence decomposition rates from fast- and slow-cycling carbon pools. In Arctic sites, where cycling rates can be very slow, radiocarbon can be used to detect changes in decomposition from millennial-cycling pools (Hicks Pries et al., 2013; Schuur et al., 2009), which strongly influence long-term carbon dynamics but may be impossible to detect with other methods. Only limited data are available of radiocarbon in ecosystem respiration or soil pore-space CO_2, particularly from Arctic sites where samples can be difficult to obtain due to low rates of CO_2 production. To characterize seasonal and spatial variations in the age of carbon pools contributing to total CO_2 efflux, we measured radiocarbon in ecosystem respiration and soil pore-space CO_2 across three summer seasons in Arctic polygon tundra.

$\Delta^{14}C$ in ecosystem respiration varied between +60.5 and -160 ‰ across the three years, with a strong seasonal trend (Fig. 1). July and August $\Delta^{14}C_{Reco}$ measurements were generally close to the $\Delta^{14}CO_2$ values of the local atmosphere, which declined from 22.2 ‰ in 2012 to 17.7 ‰ in 2014. Later in the season, we measured $\Delta^{14}CO_2$ values that differed greatly from the local atmosphere (Fig. 1), contributing ^{14}C-depleted CO_2 to the atmospheric pool. These seasonal variations in $\Delta^{14}C_{Reco}$ and respiration rates

contribute to the strong seasonal cycles of atmospheric $\Delta^{14}CO_2$ observed in the high latitudes (Graven et al., 2012). By quantifying these variations—respiration flux rates and radiocarbon values over space and time—this dataset offers useful information for atmospheric budgeting and inversions.

Measurements of soil pore-space CO_2 and late-season ecosystem respiration indicate that carbon that cycles on millennial timescales contributes substantially to soil respiration. $\Delta^{14}C_{CO2p}$ declined steeply with depth, particularly in high-centered polygons (Fig. 3); at only 20 cm below the soil surface, the mean age of carbon in the decomposition flux was as old as 3000 y (Table 2). When thaw depth approached its maximum in September and October, highly depleted ^{14}C in respiration indicated that carbon older than 1000 years was a major source of heterotrophic respiration. Together, these observations suggest that during the short summer thaw season, ancient carbon stores become available to decomposition, stabilized otherwise by cold, often frozen, and often anaerobic conditions (Mikan et al., 2002; Schmidt et al., 2011; Schuur et al., 2015).

As climate change alters these environmental controls and soils warm and thaw, a key question is how decomposition rates will change. A particularly important—but unknown—factor is the decomposition rate of carbon released from thawing permafrost (Hicks Pries et al., 2013; Koven et al., 2015; Kuhry et al., 2013). Our measurements cannot differentiate between newly thawed soil organic matter and carbon that has historically experienced an annual thaw. Our data do show, however, that when it is unfrozen, even very old Arctic soil organic carbon will readily decompose. As thaw depth progressed to the permafrost boundary, we consistently documented CO_2 production via decomposition of centennial carbon pools. As permafrost thaw progresses and Arctic soils warm, further measurements of soil-respired $^{14}CO_2$ across spatial and temporal gradients will provide critical information on soil carbon vulnerability.

Author contribution

LJSV and MST designed the sampling procedure, LJSV collected and analysed data with assistance and guidance from MST, and LJSV prepared the manuscript with contributions from MST.

Competing interests

The authors declare that they have no conflict of interest.

Acknowledgments

We thank J. Bryan Curtis and Oriana Chafe for field sampling assistance, and the Radiocarbon Collaborative for radiocarbon analyses. This research was conducted through the Next Generation Ecosystem Experiments (NGEE-Arctic) project, which is supported by the Office of Biological and Environmental Research in the US Department of Energy Office of Science.

References

ACIA: Impacts of a Warming Arctic: Arctic Climate Impact Assessment, Cambridge University Press, Cambridge, UK. [online] Available from: http://adsabs.harvard.edu/abs/2004iwaa.book.....A%EF%BF%BD%C3%9C, 2004.

Baldocchi, D.: TURNER REVIEW No. 15."Breathing" of the terrestrial biosphere: lessons learned from a global network of carbon dioxide flux measurement systems, Aust. J. Bot., 56(1), 1–26, 2008.

Billings, W. D. and Peterson, K. M.: Vegetational change and ice-wedge polygons through the thaw-lake cycle in Arctic Alaska, Arct. Alp. Res., 413–432, 1980.

Billings, W. D., Peterson, K. M. and Shaver, G. R.: Growth, Turnover, and Respiration Rates of Roots and Tillers in Tundra Graminoids, in Vegetation and Production Ecology of an Alaskan Arctic Tundra, edited by L. L. Tieszen, pp. 415–434, Springer New York., 1978.

Black, R. F.: Gubik Formation of Quaternary age in northern Alaska, United States Geological Survey. [online] Available from: http://pubs.er.usgs.gov/publication/pp302C (Accessed 29 July 2014), 1964.

Bockheim, J. G. and Tarnocai, C.: Recognition of cryoturbation for classifying permafrost-affected soils, Geoderma, 81(3–4), 281–293, doi:10.1016/S0016-7061(97)00115-8, 1998.

Bockheim, J. G., Everett, L. R., Hinkel, K. M., Nelson, F. E. and Brown, J.: Soil organic carbon storage and distribution in Arctic tundra, Barrow, Alaska, Soil Sci. Soc. Am. J., 63(4), 934–940, 1999.

Borken, W., Savage, K., Davidson, E. A. and Trumbore, S. E.: Effects of experimental drought on soil respiration and radiocarbon efflux from a temperate forest soil, Glob. Change Biol., 12(2), 177–193, doi:10.1111/j.1365-2486.2005.001058.x, 2006.

Brown, J., Miller, P. C., Tieszen, L. L. and Bunnell, F.: An Arctic ecosystem : the coastal tundra at Barrow, Alaska, Dowden, Hutchinson and Ross, Inc., Stroudsburg, Pennsylvania. [online] Available from: https://darchive.mblwhoilibrary.org/handle/1912/222 (Accessed 30 March 2014), 1980.

Chasar, L. S., Chanton, J. P., Glaser, P. H., Siegel, D. I. and Rivers, J. S.: Radiocarbon and stable carbon isotopic evidence for transport and transformation of dissolved organic carbon, dissolved inorganic carbon, and CH4 in a northern Minnesota peatland, Glob. Biogeochem. Cycles, 14(4), 1095–1108, doi:10.1029/1999GB001221, 2000.

Czimczik, C. I. and Welker, J. M.: Radiocarbon Content of CO2 Respired from High Arctic Tundra in Northwest Greenland, Arct. Antarct. Alp. Res., 42(3), 342–350, doi:10.1657/1938-4246-42.3.342, 2010.

Davidson, E. A., Savage, K., Verchot, L. V. and Navarro, R.: Minimizing artifacts and biases in chamber-based measurements of soil respiration, Agric. For. Meteorol., 113(1), 21–37, doi:10.1016/S0168-1923(02)00100-4, 2002.

Dennis, J. G.: Distribution Patterns of Belowground Standing Crop in Arctic Tundra at Barrow, Alaska, Arct. Alp. Res., 9(2), 113, doi:10.2307/1550574, 1977.

Egan, J., Nickerson, N., Phillips, C. and Risk, D.: A Numerical Examination of 14CO2 Chamber Methodologies for Sampling at the Soil Surface, Radiocarbon, 56(3), 1175–1188, doi:10.2458/56.17771, 2014.

Gaudinski, J. B., Trumbore, S. E., Davidson, E. A. and Zheng, S.: Soil carbon cycling in a temperate forest: radiocarbon-based estimates of residence times, sequestration rates and partitioning of fluxes, Biogeochemistry, 51(1), 33–69, 2000.

Graven, H. D., Guilderson, T. P. and Keeling, R. F.: Observations of radiocarbon in CO2 at seven global sampling sites in the Scripps flask network: Analysis of spatial gradients and seasonal cycles, J. Geophys. Res. Atmospheres, 117(D2) [online] Available from: http://onlinelibrary.wiley.com/doi/10.1029/2011JD016535/full (Accessed 24 May 2017), 2012.

Hahn, V., Högberg, P. and Buchmann, N.: 14C – a tool for separation of autotrophic and heterotrophic soil respiration, Glob. Change Biol., 12(6), 972–982, doi:10.1111/j.1365-2486.2006.001143.x, 2006.

Hardie, S. M. L., Garnett, M. H., Fallick, A. E., Ostle, N. J. and Rowland, A. P.: Bomb-14C analysis of ecosystem respiration reveals that peatland vegetation facilitates release of old carbon, Geoderma, 153(3), 393–401, doi:10.1016/j.geoderma.2009.09.002, 2009.

He, Y., Trumbore, S. E., Torn, M. S., Harden, J. W., Vaughn, L. J. S., Allison, S. D. and Randerson, J. T.: Radiocarbon constraints imply reduced carbon uptake by soils during the 21st century, Science, 353(6306), 1419–1424, doi:10.1126/science.aad4273, 2016.

Hicks Pries, C. E., Schuur, E. A. G. and Crummer, K. G.: Thawing permafrost increases old soil and autotrophic respiration in tundra: Partitioning ecosystem respiration using δ13C and Δ14C, Glob. Change Biol., 19(2), 649–661, doi:10.1111/gcb.12058, 2013.

Hinkel, K. M. and Nelson, F. E.: Spatial and temporal patterns of active layer thickness at Circumpolar Active Layer Monitoring (CALM) sites in northern Alaska, 1995–2000, J. Geophys. Res. Atmospheres, 108(D2), 8168, doi:10.1029/2001JD000927, 2003.

Hinkel, K. M., Paetzold, F., Nelson, F. E. and Bockheim, J. G.: Patterns of soil temperature and moisture in the active layer and upper permafrost at Barrow, Alaska: 1993–1999, Glob. Planet. Change, 29(3), 293–309, doi:10.1016/S0921-8181(01)00096-0, 2001.

Hopkins, F. M., Torn, M. S. and Trumbore, S. E.: Warming accelerates decomposition of decades-old carbon in forest soils, Proc. Natl. Acad. Sci., 109(26), E1753–E1761, doi:10.1073/pnas.1120603109, 2012.

Hubbard, S. S., Gangodagamage, C., Dafflon, B., Wainwright, H., Peterson, J., Gusmeroli, A., Ulrich, C., Wu, Y., Wilson, C., Rowland, J., Tweedie, C. and Wullschleger, S. D.: Quantifying and relating land-surface and subsurface variability in permafrost environments using LiDAR and surface geophysical datasets, Hydrogeol. J., 21(1), 149–169, doi:10.1007/s10040-012-0939-y, 2013.

Hugelius, G., Strauss, J., Zubrzycki, S., Harden, J. W., Schuur, E. A. G., Ping, C.-L., Schirrmeister, L., Grosse, G., Michaelson, G. J., Koven, C. D., O'Donnell, J. A., Elberling, B., Mishra, U., Camill, P., Yu, Z., Palmtag, J. and Kuhry, P.: Estimated stocks of circumpolar permafrost carbon with quantified uncertainty ranges and identified data gaps, Biogeosciences, 11(23), 6573–6593, doi:10.5194/bg-11-6573-2014, 2014.

Iversen, C. M., Sloan, V. L., Sullivan, P. F., Euskirchen, E. S., McGuire, A. D., Norby, R. J., Walker, A. P., Warren, J. M. and Wullschleger, S. D.: The unseen iceberg: plant roots in arctic tundra, New Phytol., 205(1), 34–58, doi:10.1111/nph.13003, 2015.

Kaiser, C., Meyer, H., Biasi, C., Rusalimova, O., Barsukov, P. and Richter, A.: Conservation of soil organic matter through cryoturbation in arctic soils in Siberia, J. Geophys. Res. Biogeosciences, 112(G2), G02017, doi:10.1029/2006JG000258, 2007.

Koven, C. D., Lawrence, D. M. and Riley, W. J.: Permafrost carbon−climate feedback is sensitive to deep soil carbon decomposability but not deep soil nitrogen dynamics, Proc. Natl. Acad. Sci., 201415123, doi:10.1073/pnas.1415123112, 2015.

Kuhry, P., Grosse, G., Harden, J. W., Hugelius, G., Koven, C. D., Ping, C.-L., Schirrmeister, L. and Tarnocai, C.: Characterisation of the Permafrost Carbon Pool, Permafr. Periglac. Process., 24(2), 146–155, doi:10.1002/ppp.1782, 2013.

Lara, M. J., McGuire, A. D., Euskirchen, E. S., Tweedie, C. E., Hinkel, K. M., Skurikhin, A. N., Romanovsky, V. E., Grosse, G., Bolton, W. R. and Genet, H.: Polygonal tundra geomorphological change in response to warming alters future CO2 and CH4 flux on the Barrow Peninsula, Glob. Change Biol., n/a-n/a, doi:10.1111/gcb.12757, 2014.

Liljedahl, A. K., Boike, J., Daanen, R. P., Fedorov, A. N., Frost, G. V., Grosse, G., Hinzman, L. D., Iijma, Y., Jorgenson, J. C., Matveyeva, N., Necsoiu, M., Raynolds, M. K., Romanovsky, V. E., Schulla, J., Tape, K. D., Walker, D. A., Wilson, C. J., Yabuki, H. and Zona, D.: Pan-Arctic ice-wedge degradation in warming permafrost and its influence on tundra hydrology, Nat. Geosci., 9(4), 312–318, doi:10.1038/ngeo2674, 2016.

Lipson, D. A., Zona, D., Raab, T. K., Bozzolo, F., Mauritz, M. and Oechel, W. C.: Water table height and microtopography control Biogeochemical cycling in an Arctic coastal tundra Ecosystem, Biogeosciences, 9, 577–591, 2012.

Loya, W. M., Johnson, L. C., Kling, G. W., King, J. Y., Reeburgh, W. S. and Nadelhoffer, K. J.: Pulse-labeling studies of carbon cycling in arctic tundra ecosystems: Contribution of photosynthates to soil organic matter, Glob. Biogeochem. Cycles, 16(4), 1101, doi:10.1029/2001GB001464, 2002.

Lupascu, M., Welker, J. M., Xu, X. and Czimczik, C. I.: Rates and radiocarbon content of summer ecosystem respiration in response to long-term deeper snow in the High Arctic of NW Greenland, J. Geophys. Res. Biogeosciences, 119(6), 2013JG002494, doi:10.1002/2013JG002494, 2014a.

Lupascu, M., Welker, J. M., Seibt, U., Xu, X., Velicogna, I., Lindsey, D. S. and Czimczik, C. I.: The amount and timing of precipitation control the magnitude, seasonality and sources (^{14}C) of ecosystem respiration in a polar semi-desert, NW Greenland, Biogeosciences Discuss., 11(2), 2457–2496, doi:10.5194/bgd-11-2457-2014, 2014b.

Meijer, H. J., Pertuisot, M. H. and Plicht, J. van der: HIGH-ACCURACY 14C MEASUREMENTS FOR ATMOSPHERIC CO2 SAMPLES BY AMS, Radiocarbon, 48(3), 355–372, 2008.

Mikan, C. J., Schimel, J. P. and Doyle, A. P.: Temperature controls of microbial respiration in arctic tundra soils above and below freezing, Soil Biol. Biochem., 34(11), 1785–1795, 2002.

Mueller, C. W., Rethemeyer, J., Kao-Kniffin, J., Löppmann, S., Hinkel, K. M. and G. Bockheim, J.: Large amounts of labile organic carbon in permafrost soils of northern Alaska, Glob. Change Biol., 21(7), 2804–2817, doi:10.1111/gcb.12876, 2015.

Norman, J. M., Kucharik, C. J., Gower, S. T., Baldocchi, D. D., Crill, P. M., Rayment, M., Savage, K. and Striegl, R. G.: A comparison of six methods for measuring soil-surface carbon dioxide fluxes, J. Geophys. Res. Atmospheres, 102(D24), 28771–28777, doi:10.1029/97JD01440, 1997.

Nowinski, N. S., Taneva, L., Trumbore, S. E. and Welker, J. M.: Decomposition of old organic matter as a result of deeper active layers in a snow depth manipulation experiment, Oecologia, 163(3), 785–792, doi:10.1007/s00442-009-1556-x, 2010.

Nydal, R. and Lövseth, K.: Carbon-14 measurements in atmospheric CO2 from northern and southern hemisphere sites, 1962-1993, Oak Ridge National Lab., TN (United States); Oak Ridge Inst. for Science and Education, TN (United States). [online] Available from: http://www.osti.gov/scitech/biblio/461185 (Accessed 24 May 2017), 1996.

Olivas, P. C., Oberbauer, S. F., Tweedie, C., Oechel, W. C., Lin, D. and Kuchy, A.: Effects of Fine-Scale Topography on CO2 Flux Components of Alaskan Coastal Plain Tundra: Response to Contrasting Growing Seasons, Arct. Antarct. Alp. Res., 43(2), 256–266, doi:10.1657/1938-4246-43.2.256, 2011.

Phillips, C. L., McFarlane, K. J., LaFranchi, B., Desai, A. R., Miller, J. B. and Lehman, S. J.: Observations of 14CO2 in ecosystem respiration from a temperate deciduous forest in Northern Wisconsin, J. Geophys. Res. Biogeosciences, 2014JG002808, doi:10.1002/2014JG002808, 2015.

Phillips, D. L. and Gregg, J. W.: Uncertainty in source partitioning using stable isotopes, Oecologia, 127(2), 171–179, doi:10.1007/s004420000578, 2001.

Ping, C. L., Bockheim, J. G., Kimble, J. M., Michaelson, G. J. and Walker, D. A.: Characteristics of cryogenic soils along a latitudinal transect in Arctic Alaska, J. Geophys. Res. Atmospheres 1984–2012, 103(D22), 28917–28928, 1998.

Randerson, J. T., Enting, I. G., Schuur, E. A. G., Caldeira, K. and Fung, I. Y.: Seasonal and latitudinal variability of troposphere Δ14CO2: Post bomb contributions from fossil fuels, oceans, the stratosphere, and the terrestrial biosphere: seasonal and latitudinal variability of trophosphere Δ14CO2, Glob. Biogeochem. Cycles, 16(4), 59-1-59–19, doi:10.1029/2002GB001876, 2002.

Reimer, P. J., Bard, E., Bayliss, A., Beck, J. W., Blackwell, P. G., Ramsey, C. B., Buck, C. E., Cheng, H., Edwards, R. L., Friedrich, M., Grootes, P. M., Guilderson, T. P., Haflidason, H., Hajdas, I., Hatté, C., Heaton, T. J., Hoffmann, D. L., Hogg, A. G., Hughen, K. A., Kaiser, K. F., Kromer, B., Manning, S. W., Niu, M., Reimer, R. W., Richards, D. A., Scott, E. M., Southon, J. R., Staff, R. A., Turney, C. S. M. and Plicht, J. van der: IntCal13 and Marine13 Radiocarbon Age Calibration Curves 0–50,000 Years cal BP, Radiocarbon, 55(4), 1869–1887, doi:10.2458/azu_js_rc.55.16947, 2013.

Schmidt, M. W., Torn, M. S., Abiven, S., Dittmar, T., Guggenberger, G., Janssens, I. A., Kleber, M., Kögel-Knabner, I., Lehmann, J. and Manning, D. A.: Persistence of soil organic matter as an ecosystem property, Nature, 478(7367), 49–56, 2011.

Schuur, E. A., Vogel, J. G., Crummer, K. G., Lee, H., Sickman, J. O. and Osterkamp, T. E.: The effect of permafrost thaw on old carbon release and net carbon exchange from tundra, Nature, 459(7246), 556–559, 2009.

Schuur, E. a. G. and Trumbore, S. E.: Partitioning sources of soil respiration in boreal black spruce forest using radiocarbon, Glob. Change Biol., 12(2), doi:10.1111/j.1365-2486.2005.01066.x, 2006.

Schuur, E. a. G., McGuire, A. D., Schädel, C., Grosse, G., Harden, J. W., Hayes, D. J., Hugelius, G., Koven, C. D., Kuhry, P., Lawrence, D. M., Natali, S. M., Olefeldt, D., Romanovsky, V. E., Schaefer, K., Turetsky, M. R., Treat, C. C. and Vonk, J. E.: Climate change and the permafrost carbon feedback, Nature, 520(7546), 171–179, doi:10.1038/nature14338, 2015.

Sierra, C. A., Müller, M., Metzler, H., Manzoni, S. and Trumbore, S. E.: The muddle of ages, turnover, transit, and residence times in the carbon cycle, Glob. Change Biol., 23(5), 1763–1773, 2017.

Strauss, J., Schirrmeister, L., Mangelsdorf, K., Eichhorn, L., Wetterich, S. and Herzschuh, U.: Organic matter quality of deep permafrost carbon – a study from Arctic Siberia, Biogeosciences Discuss, 11(11), 15945–15989, doi:10.5194/bgd-11-15945-2014, 2014.

Stuiver, M. and Polach, H. A.: Discussion reporting of 14 C data, Radiocarbon, 19(3), 355–363, 1977.

Torn, M.: CO2 CH4 flux Air temperature Soil temperature and Soil moisture, Barrow, Alaska 2013 ver. 1, Next Generation Ecosystems Experiment - Arctic, Oak Ridge National Laboratory (ORNL), Oak Ridge, TN (US)., 2015.

Torn, M., Swanston, C., Castanha, C. and Trumbore, S.: Storage and turnover of organic matter in soil, Biophys.-Chem. Process. Involv. Nat. Nonliving Org. Matter Environ. Syst., 219–272, 2009.

Trumbore, S.: Age of soil organic matter and soil respiration: radiocarbon constraints on belowground C dynamics, Ecol. Appl., 10(2), 399–411, 2000.

Trumbore, S.: Radiocarbon and soil carbon dynamics, Annu. Rev. Earth Planet. Sci., 37, 47–66, 2009.

Vaughn, L. J. S., Conrad, M. E., Bill, M. and Torn, M. S.: Isotopic insights into methane production, oxidation, and emissions in Arctic polygon tundra, Glob. Change Biol., 22(10), 3487–3502, doi:10.1111/gcb.13281, 2016.

Vaughn, L. J. S., Torn, M. S., Porras, R. C., Curtis, J. B. and Chafe, O.: Radiocarbon in Ecosystem Respiration and Soil Pore-Space CO2 with Surface Gas Flux, Air Temperature, and Soil Temperature and Moisture, Barrow, Alaska, 2012-2014, Next Generation Ecosystem Experiments Arctic Data Collection, Oak Ridge National Laboratory, U.S. Department of Energy, Oak Ridge, Tennessee, USA. [online] Available from: http://dx.doi.org/10.5440/1364062, 2018.

Wainwright, H. M., Dafflon, B., Smith, L. J., Hahn, M. S., Curtis, J. B., Wu, Y., Ulrich, C., Peterson, J. E., Torn, M. S. and Hubbard, S. S.: Identifying multiscale zonation and assessing the relative importance of polygon geomorphology on carbon fluxes in an Arctic Tundra Ecosystem, J. Geophys. Res. Biogeosciences, 2014JG002799, doi:10.1002/2014JG002799, 2015.

Waldrop, M. P., Wickland, K. P., White Iii, R., Berhe, A. A., Harden, J. W. and Romanovsky, V. E.: Molecular investigations into a globally important carbon pool: Permafrost-protected carbon in Alaskan soils, Glob. Change Biol., 16(9), 2543–2554, 2010.

Xu, L. and Baldocchi, D. D.: Seasonal variation in carbon dioxide exchange over a Mediterranean annual grassland in California, Agric. For. Meteorol., 123(1–2), 79–96, doi:10.1016/j.agrformet.2003.10.004, 2004.

Xu, L., Furtaw, M. D., Madsen, R. A., Garcia, R. L., Anderson, D. J. and McDermitt, D. K.: On maintaining pressure equilibrium between a soil CO_2 flux chamber and the ambient air, J. Geophys. Res., 111(D8), doi:10.1029/2005JD006435, 2006.

Zona, D., Gioli, B., Commane, R., Lindaas, J., Wofsy, S. C., Miller, C. E., Dinardo, S. J., Dengel, S., Sweeney, C., Karion, A. and others: Cold season emissions dominate the Arctic tundra methane budget, Proc. Natl. Acad. Sci., 113(1), 40–45, 2016.

Earth Syst. Sci. Data Discuss., https://doi.org/10.5194/essd-2018-29
Manuscript under review for journal Earth Syst. Sci. Data
Discussion started: 19 April 2018

Open Access Earth System Science Data Discussions

Table 1. Flux rate and radiocarbon abundance of soil surface CO_2 emissions with associated thaw depth and temperature measurements

Profile	Date	Thaw depth (cm)	Air temp °C	5cm soil temp* °C	10cm soil temp* °C	CO_2 flux** (μmol m^{-2} d^{-1})	^{14}C Analysis year	$F^{14}C$	$\Delta^{14}C_{CO2}$*** (‰)
HC1-center	8/9/12	31	--	5.9 ± 0.0	4.3 ± 0.0	--	2013	1.0298	-58.4 ± 6.1
	9/2/14	32	4.6	4.3 ± 0.6	3.3 ± 0.5	0.547 ± 0.0047	2016	0.8916	-115.5 ± 10.2
HC1-rim	10/6/12	--	-1.0	1.4	1.6	--	2013	1.0298	22.0 ± 4.1
HC1-trough	8/8/12	--	--	--	--	--	2017	1.0420	33.6 ± 3.5
	8/11/12	32	--	6.3 ± 0.6	4.6 ± 0.2	--	2017	1.0501	41.6 ± 4.1
	10/6/12	--	-1.0	1.4	1.5	--	2013	0.9936	-14.0 ± 3.2
	9/6/13	36	0.5	0.85 ± 0.07	0.85 ± 0.16 (n=3)	1.53 ± 0.016	2013	1.0271	19.3 ± 3.6
HC2-center	9/7/14	23	4.0	3.4 ± 0.1	2.3 ± 0.	0.425 ± 0.0038	2016	0.9775	-31.3 ± 5.0
HC3-center	8/13/12	29	9.7	11.7 ± 1.1 (n=4)	9.8 ± 1.6 (n=4)	--	2013	1.0408	32.9 ± 5.2
	9/7/14	31	4.0	2.8 ± 0.2	2.4 ± 0.4	0.408 ± 0.0043	2017	0.9991	-9.0 ± 1.9
HC3-trough	7/12/13	--	10	--	--	1.65 ± 0.0070	2013	1.0520	44.0 ± 6.0
	9/6/13	32	4.0	--	3.1 ± 0.2 (n=3)	0.489 ± 0.0033	2013	1.0211	13.3 ± 3.7
FC1-center	9/2/14	37	5.3	4.3 ± 1.5	2.9 ± 0.1	0.572 ± 0.0066	2016	1.0044	-3.6 ± 2.9
FC2-rim	8/12/12	29	--	4.7 ± 0.4	3.9 ± 0.2	--	2017	1.0343	25.9 ± 2.5
	10/6/12	--	-1.0	--	--	--	2013	1.0375	29.7 ± 3.3
FC2-trough	8/11/12	27	--	3.7 ± 0.5	2.8 ± 0.2	--	2017	1.0428	34.3 ± 3.4
	7/14/13	25	9.8	3.3 ± 0.1 (n=3)	2.3 ± 0.2 (n=3)	2.47 ± 0.011	2013	1.0372	29.3 ± 3.7
	9/6/13	30	3.2	2.1 ± 1.6 (n=3)	1.5 ± 0.4 (n=3)	1.50 ± 0.0076	2013	1.0171	9.4 ± 3.6
FC3-center	9/2/14	44	4.5	3.5 ± 0.2	2.8 ± 0.1	0.464 ± 0.0043	2016	1.0173	9.2 ± 3.6
FC4-center	9/7/14	34	2.0	2.4 ± 0.8	1.8 ± 0.7	0.312 ± 0.0032	2016	1.0418	33.5 ± 4.1
FC4-trough	9/5/13	36	5.2	--	4.4 ± 0.6 (n=3)	0.471 ± 0.0029	2013	1.0163	8.6 ± 3.9
LC1-center	8/10/12	31	--	5.7 ± 0.07	4.3 ± 0.07	--	2017	1.0317	23.3 ± 2.5
	10/6/12	--	-1.0	1.9	1.9	--	2013	0.8470	-159.5 ± 13.1
	9/7/13	34	3.2	--	2.1 ± 0.2 (n=3)	0.825 ± 0.0092	2013	1.0026	-5.0 ± 4.4
LC1-rim	10/6/12	--	-1.0	1.8	1.9	--	2013	1.0663	58.2 ± 7.3
LC1-trough	8/10/12	33	--	5.5 ± 2.3	4.1 ± 1.5	--	2017	1.0464	40.0 ± 3.7
	10/6/12	--	-1.0	1.9	2.1	--	2013	1.0339	26.1 ± 6.5
	9/7/13	41	3.2	--	2.7 ± 0.3 (n=3)	0.320 ± 0.0033	2013	1.0389	31.0 ± 4.6
LC2-center	9/2/14	29	4.8	5.2 ± 0.1	4.3 ± 0.1	0.372 ± 0.0032	2016	1.0221	14.0 ± 3.8
LC3-center	10/6/12	--	-1.0	1.7 ± 0.2	1.6 ± 0.07	--	2013	1.0304	22.5 ± 3.4
	7/12/13	23	8.2	12.9 ± 0.04	8.8 ± 0.2	0.607 ± 0.0032	2013	1.0336	25.8 ± 3.6
	9/7/13	33	2.0	--	2.5 ± 0.02 (n=3)	1.12 ± 0.019	2013	1.0386	30.7 ± 4.2
	9/2/14	27	5.0	5.1 ± 0.1	4.3 ± 0.0	0.521 ± 0.0023	2016	1.0167	8.6 ± 3.7
LC3-trough	10/6/12	--	-1.0	--	--	--	2013	1.0686	60.5 ± 9.8
	7/12/13	31	8.2	10.5 ± 0.4	6.6 ± 0.08	0.674 ± 0.0021	2013	1.0445	36.5 ± 4.1
	9/7/13	37	2.0	--	2.3 ± 0.2 (n=3)	1.31 ± 0.0046	2013	1.0686	27.3 ± 4.1
LC4-center	9/7/14	28	3.1	7.1 ± 0.3	6.1 ± 0.9	0.463 ± 0.0029	2016	1.0031	-4.9 ± 3.8

Note: -- indicates measurements for which data are unavailable.

*Error ranges represent standard deviations across measurements with n=2 unless otherwise noted. When only one measurement was made, no error range is reported.

**Error ranges represent standard error of the regression used to calculate CO_2 flux.

***Values have been corrected to exclude atmospheric CO_2 using a 2-pool isotopic mixing model. Error ranges represent standard errors from the 2-pool mixing model, derived from analytical error and standard deviations in the source isotopic compositions.

Earth Syst. Sci. Data Discuss., https://doi.org/10.5194/essd-2018-29
Manuscript under review for journal Earth Syst. Sci. Data
Discussion started: 19 April 2018

Open Access Earth System Science Data Discussions

Table 2. Isotopic composition of soil profile CO_2

Profile	Month	Depth (cm)	$\delta^{13}C_{CO2}$ (‰)	Analysis year	$F^{14}C$	$\Delta^{14}C_{CO2}$ (‰)	Mean age of respired C (y)
HC1-center	8/2012	31	--	2013	0.7464	-259.2 ± 7.5	3050
	9/2013	20	-23.7	2013	0.7270	-278.6 ± 2.6	3350
HC3-center	8/2012	10	-20.1	2013	0.9473	-59.9 ± 3.0	770
	8/2012	20	--	2013	0.8864	-120.3 ± 3.2	1320
	8/2012	29	-21.7	2013	0.8944	-112.4 ± 2.7	1240
	7/2013	10	--	2013	0.9037	-101.3 ± 4.4	1150
	7/2013	20	--	2013	0.7382	-267.4 ± 2.6	3170
HC3-trough	7/2013	10	--	2013	0.7898	-216.2 ± 3.3	2440
	7/2013	20	-23.7	2013	0.8447	-161.7 ± 2.4	1760
FC2-center	8/2012	10	-24.8	2013	0.9509	-56.3 ± 2.8	740
	8/2012	20	-24.9	2013	0.9729	-34.5 ± 2.9	580
FC4-center	7/2013	20	-24.8	2013	0.8034	-202.7 ± 2.1	2260
LC3-trough	7/2013	10	-24.7	2013	1.0005	-7.1 ± 3.9	410
	7/2013	20	--	2013	0.8755	-131.2 ± 3.7	1430

Earth Syst. Sci. Data Discuss., https://doi.org/10.5194/essd-2018-29
Manuscript under review for journal Earth Syst. Sci. Data
Discussion started: 19 April 2018

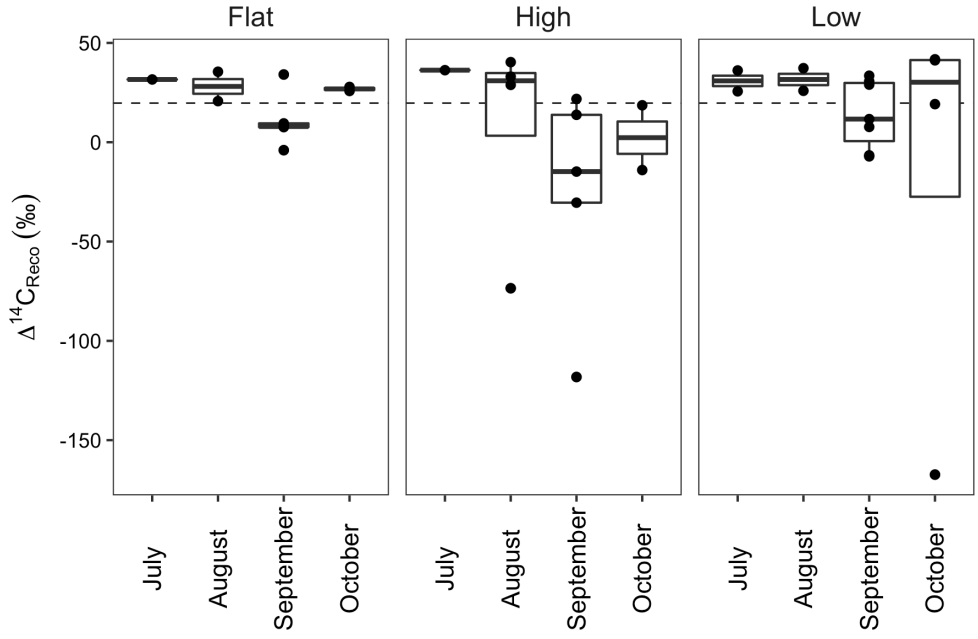

Figure 1. Radiocarbon content of ecosystem respiration, separated by polygon type and sampling month. Boxes represent the first and third quartiles, and whiskers extend to the farthest values within 1.5 times this range. Dashed horizontal line indicates the mean $\Delta^{14}C$-CO_2 of the local atmosphere during the 2012-2014 summer seasons.

Earth Syst. Sci. Data Discuss., https://doi.org/10.5194/essd-2018-29
Manuscript under review for journal Earth Syst. Sci. Data
Discussion started: 19 April 2018

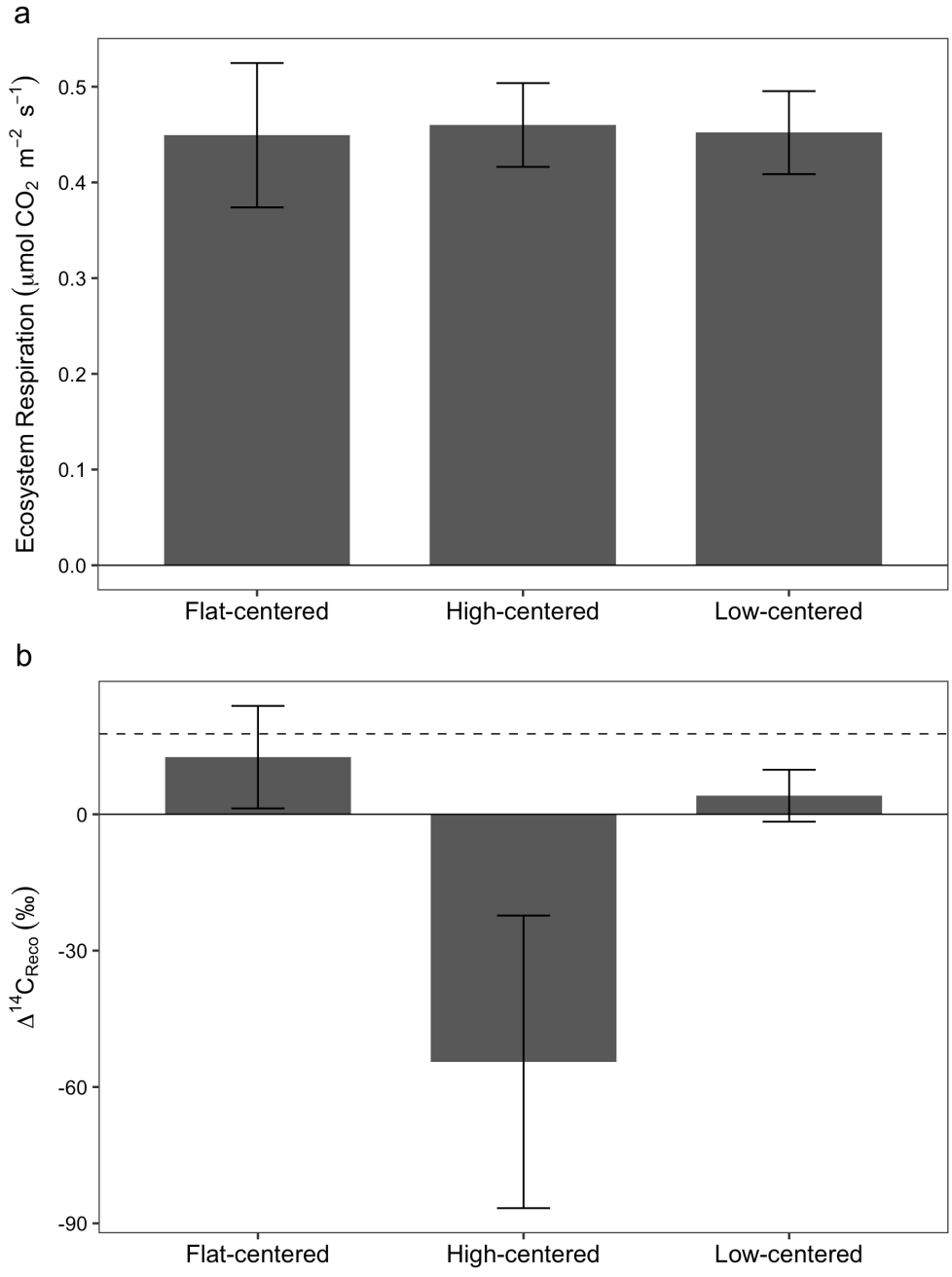

Figure 2. Ecosystem respiration rate (a) and radiocarbon content (b), measured from polygon centers in September 2014. Error bars represent standard error with n=3. Dashed horizontal line indicates $\Delta^{14}C\text{-}CO_2$ of the local atmosphere at the time of sampling.

Earth Syst. Sci. Data Discuss., https://doi.org/10.5194/essd-2018-29
Manuscript under review for journal Earth Syst. Sci. Data
Discussion started: 19 April 2018

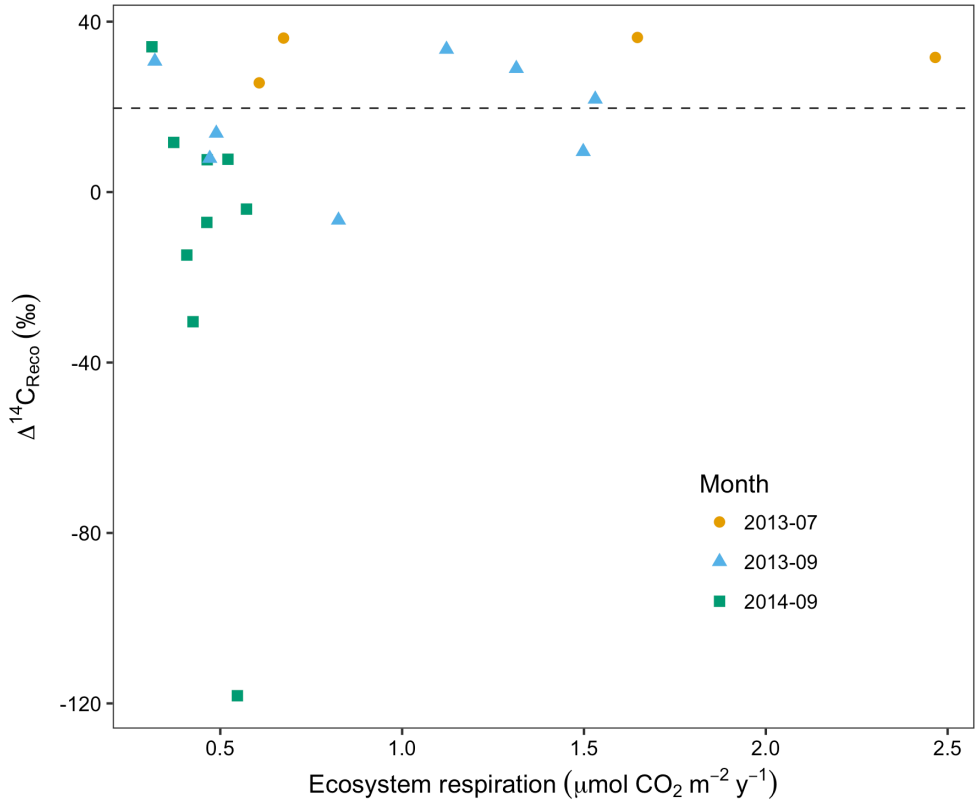

Figure 3. Rates and radiocarbon contents of ecosystem respiration in July and September 2013 and September 2014. Dashed horizontal line indicates the mean $\Delta^{14}C$-CO_2 of the local atmosphere during the 2013 and 2014 summer seasons.

Earth Syst. Sci. Data Discuss., https://doi.org/10.5194/essd-2018-29
Manuscript under review for journal Earth Syst. Sci. Data
Discussion started: 19 April 2018

Open Access Earth System Science Data Discussions

5

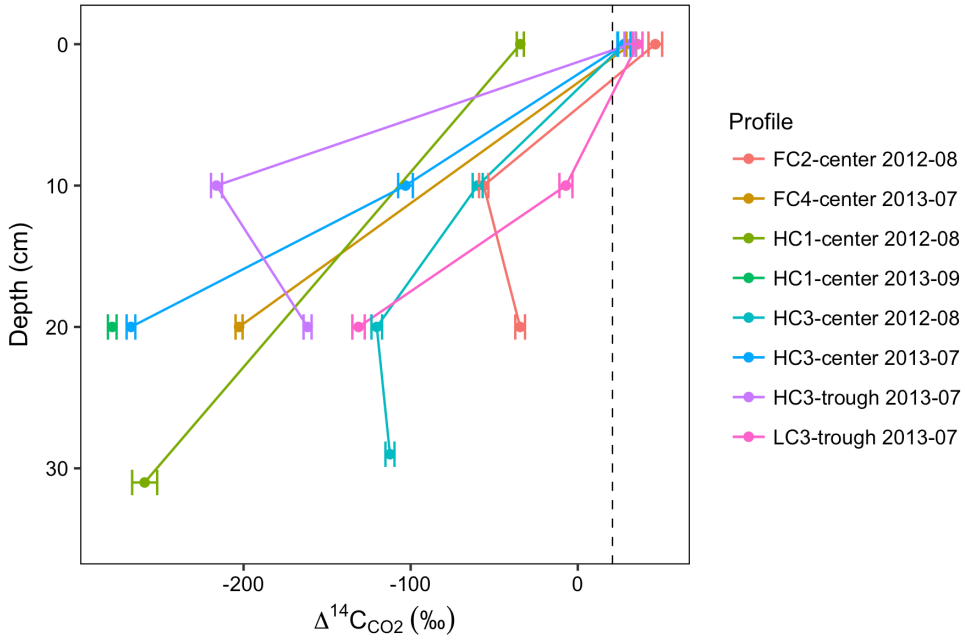

Figure 4. Soil depth profiles of $\Delta^{14}C$-CO_2. Lines connect samples collected in the same vertical profile and month, and error bars represent analytical error. Samples from 0 cm depth were collected from surface soil chambers and reflect CO_2 that accumulated after chambers were scrubbed of CO_2. All other samples were collected from soil wells. Dashed vertical line indicates the mean $\Delta^{14}C$-CO_2 of the local atmosphere during the 2012 and 2013 summer seasons.

10